

Volume 2, Issue 1

Research Article

Date of Submission: 20 November, 2025

Date of Acceptance: 30 January, 2026

Date of Publication: 09 February, 2026

Analysis and Control of an Acetaminophen Metabolism Dynamic Model

Lakshmi N. Sridhar*

Chemical Engineering Department, University of Puerto Rico Mayaguez, USA

*Corresponding Author:

Lakshmi N. Sridhar, Chemical Engineering Department, University of Puerto Rico Mayaguez, USA.

Citation: Sridhar, L. N. (2026). Analysis and Control of an Acetaminophen Metabolism Dynamic Model. *J Bioeng Appl Biosci*, 2(1), 01-12.

Abstract

In this study, bifurcation analysis and multi-objective nonlinear model predictive control are performed on an Acetaminophen Metabolism dynamic model. Bifurcation analysis is a powerful mathematical tool used to deal with the nonlinear dynamics of any process. Several factors must be considered, and multiple objectives must be met simultaneously.

The MATLAB program MATCONT was used to perform the bifurcation analysis. The MNLMPC calculations were performed using the optimization language PYOMO in conjunction with the state-of-the-art global optimization solvers IPOPT and BARON. The bifurcation analysis revealed branch and limit points. The MNLMC converged on the utopia solution. The branch points (which cause multiple steady-state solutions from a singular point) are very beneficial because they enable the multiobjective nonlinear model predictive control calculations to converge to the Utopia point (the best possible solution) in the model.

Keywords: Bifurcation, Optimization, Control, Acetaminophen, Metabolism

Background

Acetaminophen, also known as paracetamol, is one of the most commonly used analgesics and antipyretics worldwide. Its metabolism is complex, involving several enzymatic pathways in the liver, which play a crucial role in both its therapeutic effects and the potential risks associated with overdose. Acetaminophen undergoes extensive metabolism in the liver, where it is primarily converted into non-toxic metabolites, but a small proportion is also metabolized into a toxic intermediate, which can lead to liver damage when it accumulates at high concentrations.

When acetaminophen is absorbed into the bloodstream after oral administration, it is transported to the liver, where its metabolism takes place predominantly through three main pathways: conjugation with sulfate, conjugation with glucuronic acid, and oxidation by the cytochrome P450 enzyme system. The majority of acetaminophen (about 90%) undergoes phase II metabolism, where it is conjugated with sulfate or glucuronic acid to form water-soluble metabolites that are readily excreted in the urine. These conjugates are essentially non-toxic and are the main products excreted after normal doses.

However, a small fraction of acetaminophen (approximately 5–10%) is metabolized by the cytochrome P450 enzymes, specifically CYP2E1, CYP1A2, and CYP3A4. This process generates a highly reactive intermediate known as N-acetyl-p-benzoquinone imine (NAPQI). Under normal conditions, NAPQI is quickly neutralized by conjugation with glutathione, a tripeptide antioxidant found in the liver. This results in the formation of non-toxic metabolites that are safely excreted from the body. However, if the dose of acetaminophen is excessively high, the available stores of glutathione become

depleted, and NAPQI accumulates in the liver. This accumulation can lead to oxidative damage to liver cells, ultimately causing liver injury and, in severe cases, acute liver failure.

The risk of liver toxicity is significantly increased in cases of acetaminophen overdose, particularly when the dose exceeds 4 grams per day for adults, or when multiple doses are taken over a short period. Factors such as chronic alcohol consumption, malnutrition, or the use of drugs that induce cytochrome P450 enzymes (such as certain anticonvulsants) can exacerbate the formation of NAPQI by increasing the activity of these enzymes. In these situations, even normal therapeutic doses of acetaminophen may pose a greater risk for liver damage, as the body's capacity to detoxify NAPQI is overwhelmed. Treatment for acetaminophen overdose primarily focuses on replenishing glutathione levels to help neutralize the toxic metabolite. N-acetylcysteine (NAC) is the most common antidote and acts by providing cysteine, a precursor to glutathione, which helps restore the body's ability to detoxify NAPQI. When administered early, NAC can significantly reduce the risk of liver injury and improve outcomes in cases of overdose.

Despite its potential for toxicity, acetaminophen is widely regarded as a safe and effective analgesic when used at recommended doses. Its metabolism in the liver is generally well-tolerated in healthy individuals, but understanding the pathways and risks involved is essential to minimizing harm. Moreover, awareness of the factors that increase the risk of toxicity can help clinicians provide better care to individuals who are at higher risk, ensuring that acetaminophen is used safely in both acute and chronic settings.

Mutlib et al (2006) studied the kinetics of acetaminophen glucuronidation by UDP-glucuronosyltransferases [1]. Reed et al (2008), developed a mathematical model of glutathione metabolism [2]. Reith et al (2009) performed modelling of the Michaelis-Menten Kinetics of Paracetamol sulfate and Glucuronidation [3]. Trinh et al (2009) developed "elementary mode analysis," a useful metabolic pathway analysis tool for characterizing cellular metabolism [4]. Ben-Shachar et al (2012) studied the biochemistry of acetaminophen hepatotoxicity and rescue using a mathematical model [5]. Remien et al (2012) modelled liver injury and dysfunction after acetaminophen overdose, focusing on early discrimination between survival and death [6]. Reddyhoff et al (2015) provided a timescale analysis of a mathematical model of acetaminophen metabolism and toxicity [7].

Ghosh(2021), studied the role of alcohol consumption on acetaminophen-induced liver injury identifying the implications from a mathematical model [8]. Sankarraman (2022) developed a computational approach on the acetaminophen drug using degree-based topological indices and m-polynomials [9]. Belmont-Díaz et al(2022) developed a metabolic control analysis for drug Target Selection against human diseases [10]. Yoo et al (2023) studied acetaminophen adsorption to spherical carbons hydrothermally synthesized from sucrose [11]. Dichamp et al(2023) investigated In vitro to in vivo acetaminophen hepatotoxicity extrapolation using classical schemes, pharmacodynamic models and a multiscale spatial-temporal liver twin [12]. Zahwa et al (2025) developed optimal control strategies for reducing toxic formation in Acetaminophen metabolism [13].

This work aims to perform bifurcation analysis and multiobjective nonlinear control (MNL MPC) studies on an Acetaminophen metabolism dynamic model [13]. The paper is organized as follows. First, the model equations are presented, followed by a discussion of the numerical techniques involving bifurcation analysis and multiobjective nonlinear model predictive control (MNL MPC). The results are then presented, followed by the discussion and conclusions.

Model Equations

The variables $s_1, s_2, s_3, s_4, s_5, s_6, s_7, s_8, s_9$ represent the Acetaminophen(APAP) in the gut; APAP in the liver; Phosphoadenosine-5-phosphosulfate (PAPS) in the liver; APAP Sulfate (APAP-S) in the liver; APAP Glucuronidate (APAP-G) in the liver; NAPQI in the liver; the antioxidant GSH in the liver; NAPQIGSH in the liver; and the living cells in the liver.

The variables p_1, p_2, p_3, p_4 are given by

$$\begin{aligned}
 p_1 &= (v_1(1-u_1) \frac{s_2}{(km_1+s_2)} + v_2(1-u_1) \frac{s_2}{(km_2+s_2)} + (v_3(1-u_1) \frac{s_2}{(km_3+s_2)} /)) (1 + (pp(\frac{s_2^{np}}{((d^{np}) + (s_2^{np})))))) \\
 p_2 &= \frac{v_4 s_2 s_3}{(ks_1 t + (km_4 s_2) + (km_5 s_3) + (s_2 s_3))} \\
 p_3 &= \frac{v_5(1-u_2) s_2^{mp}}{(km_6^m p + s_2^{mp})} / + \frac{v_6(1-u_2) s_2}{(km_7 + s_2(1 + (\frac{s_2}{ki_7})))} + \frac{v_7(1-u_2) s_2}{(km_8 + s_2)} + \frac{v_8(1-u_2) s_2}{(km_9 + s_2(1 + (\frac{s_2}{ki_9})))} \\
 p_4 &= \frac{v_9 s_6 s_7}{(kgsh + (km_{10} * s_6) + (km_{11} * s_7) + (s_6 * s_7))} \tag{1}
 \end{aligned}$$

The Differential Equations are Given by

$$\begin{aligned}
 \frac{ds_1}{dt} &= -kal(s_1) \\
 \frac{ds_2}{dt} &= kal(s_1) - p_1 - p_2 - p_3 \\
 \frac{ds_3}{dt} &= -p_2 - (ds(s_3)) \\
 \frac{ds_4}{dt} &= p_2 + bs - (ksl(s_4)) \\
 \frac{ds_5}{dt} &= p_3 - (kgl(s_5)) \\
 \frac{ds_6}{dt} &= p_1 - p_4 - (\eta(s_6)s_9) \\
 \frac{ds_7}{dt} &= -p_4 + bg - (dg(s_7)) \\
 \frac{ds_8}{dt} &= p_4 - (knqgl(s_8)) \\
 \frac{ds_9}{dt} &= \left(r(s_9) \left(1 - \left(\frac{s_9}{h_{\max}} \right) \right) \right) - (\eta(s_6)s_9) - \delta(s_9)
 \end{aligned} \tag{2}$$

The Variable Values Are

kal=4; km9=23000; kgl=0.81; ksl=0.24; km11=4600; kgsh=1.87e-03; knqgl=0.29; ki9=5300; kslt=13.27; bg=0.07; d=18000; mp=3; dg=0.08; ds=0.08; bs=0.13; v1=0.55; v3=0.99; v4=1785; v7=4900; =0.21e-04; u1=0; u2=0; r=0.04; km10=15; =0.08; km1=3430; ki7=23000; km2=677; km3=276; pp=20; km4=97; km5=3.3e-03; np=2; hmax=1.6e+11; km6=5500; km7=4000; km8=9200; v2=345; v6=490; v5=6370; v8=8820; v9=72000. Details of the model parameters and other model details are in Zahwa et al (2025).

Bifurcation Analysis

Bifurcation analysis deals with multiple steady-states (caused by branch and limit points) and limit cycles, which are caused by Hopf bifurcation points. The MATLAB program MATCONT is used to locate limit points, branch points, and Hopf bifurcation points [14,15]. In ODE system

$$\frac{dx}{dt} = f(x, \alpha) \tag{3}$$

$x \in R^n$ Let the bifurcation parameter be α . Since the gradient is orthogonal to the tangent vector, The tangent plane is the $n+1$ -dimensional vector w that satisfies

$$Aw = 0 \tag{4}$$

Where A is

$$A = [\partial f / \partial x \quad | \quad \partial f / \partial \alpha] \tag{5}$$

And $\partial f / \partial x$ is the Jacobian matrix. For both limit and branch points, the Jacobian matrix $J = [\partial f / \partial x]$ must be singular. For a limit point, there is only one tangent at the point of singularity. At this singular point, there is a single non-zero vector, y , where $Jy=0$. This vector is of dimension n . Since there is only one tangent the vector $y = (y_1, y_2, y_3, y_4, \dots, y_n)$ must align with $\hat{w} = (w_1, w_2, w_3, w_4, \dots, w_n)$. Since

$$J\hat{w} = Aw = 0 \tag{6}$$

the $n+1$ th component of the tangent vector $w_{n+1} = 0$ at a limit point (LP).

For a branch point, there must exist two tangents at the singularity. Let the two tangents be z and w . This implies that

$$\begin{aligned} Az &= 0 \\ Aw &= 0 \end{aligned} \tag{7}$$

Consider a vector v that is orthogonal to one of the tangents (say w). v can be expressed as a linear combination of z and w ($v = \alpha z + \beta w$). Since $Az = Aw = 0$; $Av = 0$ and since w and v are orthogonal,

$$w^T v = 0. \text{ Hence } Bv = \begin{bmatrix} A \\ w^T \end{bmatrix} v = 0 \text{ which implies that } B \text{ is singular.}$$

Hence, the matrix $B = \begin{bmatrix} A \\ w^T \end{bmatrix}$ is singular at a branch point.

When there is a Hopf bifurcation point the bialternate product,

$$\det(2f_x(x, \alpha) @ Jn) = 0 \tag{8}$$

where Jn is the n -square identity matrix. Hopf bifurcations cause limit cycles and should be eliminated because limit cycles make optimization and control tasks very difficult. More details can be found in Kuznetsov (1998; 2009) and Govaerts [2000] [16-18].

Multiobjective Nonlinear Model Predictive Control(MNLMPC)

The rigorous multiobjective nonlinear model predictive control (MNLMPC) method developed by Flores Tlacuahuaz et al (2012) was used [19]. Consider a problem where the variables $\sum_{t_i=0}^{t_i=t_f} q_j(t_i)$ have to be optimized together for a dynamic problem

$$\frac{dx}{dt} = F(x, u) \tag{9}$$

t_f being the final time value and u the control parameter. The individual objective optimal control problem is solved

by optimizing each of the variables $\sum_{t_i=0}^{t_i=t_f} q_j(t_i)$. The optimization of $\sum_{t_i=0}^{t_i=t_f} q_j(t_i)$ will lead to the values q_j^* . Then the

multiobjective optimal control (MOOC)problem

$$\begin{aligned} \min & \left(\sum_{j=1}^n \left(\sum_{t_i=0}^{t_i=t_f} q_j(t_i) - q_j^* \right) \right)^2 \\ \text{subject to} & \frac{dx}{dt} = F(x, u); \end{aligned} \tag{10}$$

is solved. This will provide the value of u at each time step. The first obtained control value of u is implemented and this procedure is repeated until the implemented and the first obtained control values are the same or where

$\left(\sum_{t_i=0}^{t_i=t_f} q_j(t_i) - q_j^* \right) = 0$ for all j . Utopia point) is obtained. The optimization program PYOMO is used [20]. Here, the

differential equations are converted to a Nonlinear Program (NLP) using the orthogonal collocation method. The NLP is solved using IPOPT and confirmed as a global solution with BARON [21,22].

The Steps of the Algorithm are as Follows

- Optimize $\sum_{t_i=0}^{t_i=t_f} q_j(t_i)$ and obtain q_j^* .

- Minimize $(\sum_{j=1}^n (\sum_{t_i=0}^{t_i=t_f} q_j(t_i) - q_j^*))^2$ and get the control values at various times.
- Implement the first obtained control values
- Repeat steps 1 to 3 until there is an insignificant difference between the implemented and the first obtained value of the control variables or if the Utopia point is achieved. The Utopia point is when $\sum_{t_i=0}^{t_i=t_f} q_j(t_i) - q_j^* = 0$ for all j.

Sridhar (2024) demonstrated that when the bifurcation analysis revealed the presence of limit and branch points the MNLMPMC calculations to converge to the Utopia solution [23]. For this, the singularity condition, caused by the presence of the limit or branch points was imposed on the co-state equation [24]. If the minimization of q_1 lead to the value q_1^* and the minimization of q_2 lead to the value q_2^* The MNLMPMC calculations will minimize the function $(q_1 - q_1^*)^2 + (q_2 - q_2^*)^2$. The multiobjective optimal control problem is

$$\min (q_1 - q_1^*)^2 + (q_2 - q_2^*)^2 \quad \text{subject to} \quad \frac{dx}{dt} = F(x, u) \quad (11)$$

Differentiating the objective function results in

$$\frac{d}{dx_i} ((q_1 - q_1^*)^2 + (q_2 - q_2^*)^2) = 2(q_1 - q_1^*) \frac{d}{dx_i} (q_1 - q_1^*) + 2(q_2 - q_2^*) \frac{d}{dx_i} (q_2 - q_2^*) \quad (12)$$

The Utopia point requires that both $(q_1 - q_1^*)$ and $(q_2 - q_2^*)$ are zero. Hence

$$\frac{d}{dx_i} ((q_1 - q_1^*)^2 + (q_2 - q_2^*)^2) = 0 \quad (13)$$

The optimal control co-state equation (Upreti; 2013)[33] is

$$\frac{d}{dt} (\lambda_i) = -\frac{d}{dx_i} ((q_1 - q_1^*)^2 + (q_2 - q_2^*)^2) - f_x \lambda_i; \quad \lambda_i(t_f) = 0 \quad (14)$$

λ_i is the Lagrangian multiplier. t_f is the final time. The first term in this equation is 0 and hence

$$\frac{d}{dt} (\lambda_i) = -f_x \lambda_i; \lambda_i(t_f) = 0 \quad (15)$$

At a limit or a branch point, for the set of ODE $\frac{dx}{dt} = f(x, u)$ f_x is singular. Hence there are two different vectors-values for $[\lambda_i]$ where $\frac{d}{dt} (\lambda_i) > 0$ and $\frac{d}{dt} (\lambda_i) < 0$. In between there is a vector $[\lambda_i]$ where $\frac{d}{dt} (\lambda_i) = 0$. This coupled

with the boundary condition $\lambda_i(t_f) = 0$ will lead to $[\lambda_i] = 0$ This makes the problem an unconstrained optimization problem, and the optimal solution is the Utopia solution.

Results and Discussion

Theorem

If one of the functions in a dynamic system is separable into two distinct functions, a branch point singularity will occur in the system.

Proof

Consider a system of equations

$$\frac{dx}{dt} = f(x, \alpha) \quad (16)$$

$x \in R^n$. Defining the matrix A as

$$A = \begin{bmatrix} \frac{\partial f_1}{\partial x_1} & \frac{\partial f_1}{\partial x_2} & \frac{\partial f_1}{\partial x_3} & \frac{\partial f_1}{\partial x_4} & \dots & \frac{\partial f_1}{\partial x_n} & \frac{\partial f_1}{\partial \alpha} \\ \frac{\partial f_2}{\partial x_1} & \frac{\partial f_2}{\partial x_2} & \frac{\partial f_2}{\partial x_3} & \frac{\partial f_2}{\partial x_4} & \dots & \frac{\partial f_2}{\partial x_n} & \frac{\partial f_2}{\partial \alpha} \\ \dots & \dots & \dots & \dots & \dots & \dots & \dots \\ \frac{\partial f_n}{\partial x_1} & \frac{\partial f_n}{\partial x_2} & \frac{\partial f_n}{\partial x_3} & \frac{\partial f_n}{\partial x_4} & \dots & \frac{\partial f_n}{\partial x_n} & \frac{\partial f_n}{\partial \alpha} \end{bmatrix} \quad (17)$$

α is the bifurcation parameter. The matrix A can be written in a compact form as

$$A = \left[\frac{\partial f_p}{\partial x_q} \cdot \mid \frac{\partial f_p}{\partial \alpha} \right] \quad (18)$$

The tangent at any point x ; ($z = [z_1, z_2, z_3, z_4, \dots, z_{n+1}]$) must satisfy

$$Az = 0 \quad (19)$$

The matrix $\left\{ \frac{\partial f_p}{\partial x_q} \right\}$ must be singular at both limit and branch points. The $n+1$ th component of the tangent vector z_{n+1}

= 0 at a limit point (LP) and for a branch point (BP) the matrix $B = \begin{bmatrix} A \\ z^T \end{bmatrix}$ must be singular. Any tangent at a point y that is defined by $z = [z_1, z_2, z_3, z_4, \dots, z_{n+1}]$ must satisfy

$$Az = 0 \quad (20)$$

For a branch point, there must exist two tangents at the singularity. Let the two tangents be z and w . This implies that

$$\begin{aligned} Az &= 0 \\ Aw &= 0 \end{aligned} \quad (21)$$

Consider a vector v that is orthogonal to one of the tangents (say z). v can be expressed as a linear combination of z and w ($v = \alpha z + \beta w$). Since $Az = Aw = 0$; $Av = 0$ and since z and v are orthogonal,

$$z^T v = 0. \text{ Hence } Bv = \begin{bmatrix} A \\ z^T \end{bmatrix} v = 0 \text{ which implies that B is singular where } B = \begin{bmatrix} A \\ z^T \end{bmatrix}$$

Let any of the functions f_i are separable into 2 functions ϕ_1, ϕ_2 as

$$f_i = \phi_1 \phi_2 \quad (22)$$

At steady-state $f_i(x, \alpha) = 0$ and this will imply that either $\phi_1 = 0$ or $\phi_2 = 0$ or both ϕ_1 and ϕ_2 must be 0. This implies that two branches $\phi_1 = 0$ and $\phi_2 = 0$ will meet at a point where both ϕ_1 and ϕ_2 are 0. At this point, the matrix B will be singular as a row in this matrix would be

$$\left[\frac{\partial f_i}{\partial x_k} \mid \frac{\partial f_i}{\partial \alpha} \right] \quad (23)$$

However,

$$\begin{aligned} \left[\frac{\partial f_i}{\partial x_k} = \phi_1(=0) \frac{\partial \phi_2}{\partial x_k} + \phi_2(=0) \frac{\partial \phi_1}{\partial x_k} = 0 (\forall k = 1, \dots, n) \right. \\ \left. \frac{\partial f_i}{\partial \alpha} = \phi_1(=0) \frac{\partial \phi_2}{\partial \alpha} + \phi_2(=0) \frac{\partial \phi_1}{\partial \alpha} \right] = 0 \end{aligned} \quad (24)$$

This implies that every element in the row $\left[\frac{\partial f_i}{\partial x_k} \mid \frac{\partial f_i}{\partial \alpha} \right]$ would be 0, and hence the matrix B would be singular. The singularity in B implies that there exists a branch point.

Bifurcation Results

When δ is the bifurcation parameter; the branch point occurs at $(s_1, s_2, s_3, s_4, s_5, s_6, s_7, s_8, s_9, \delta)$ values of $(0, 0, 0, 0.541667, 0, 0, 0.875, 0, 0, 0.04)$ (Fig. 1a). Here, the two distinct functions can be obtained from the first ODE in the model

$$\frac{ds_9}{dt} = \left(r(s_9) \left(1 - \left(\frac{s_9}{h_{\max}} \right) \right) \right) - (\eta(s_6)s_9) - \delta(s_9) \quad (25)$$

The two distinct equations are

$$\begin{aligned} s_9 = 0 \\ \left(r \left(1 - \left(\frac{s_9}{h_{\max}} \right) \right) \right) - (\eta(s_6)) - \delta \end{aligned} \quad (26)$$

With $s_9=0$; $s_6=0$; $r=0.04$; $\delta=0.04$, both distinct equations are satisfied, validating the theorem. Additionally, two limit points were observed at $(s_1, s_2, s_3, s_4, s_5, s_6, s_7, s_8, s_9, \delta)$ values of $(0, 0, 0, 0.541667, 0, 0, 0.875, 0, 0.79, 0.04)$ and $(0, 0, 0, 0.541667, 0, 0, 0.875, 0, 1.29, 0.04)$. These limit points are also seen in Figure 1a.

When u_1 is the bifurcation parameter, a branch point is seen at $(s_1, s_2, s_3, s_4, s_5, s_6, s_7, s_8, s_9, u_1)$ values of $(0, 0, 0, 0.541667, 0, 0, 0.875, 0, 0, 3.023162)$ (Figure 1b).

When u_2 is the bifurcation parameter, a branch point is seen at $(s_1, s_2, s_3, s_4, s_5, s_6, s_7, s_8, s_9, u_2)$ values of $(0, 0, 0, 0.541667, 0, 0, 0.875, 0, 0, 1.494276)$ (Figure 1c).

For the MNLMPC, u_1, u_2 are the control parameters, and $\sum_{t_i=0}^{t_i=t_f} s_7(t_i)$ is maximized and $\sum_{t_i=0}^{t_i=t_f} s_6(t_i)$ is minimized individually, and led to values of 14.975 and 0. The overall optimal control problem will involve the minimization of $\left(\sum_{t_i=0}^{t_i=t_f} s_7(t_i) - 14.975 \right)^2 + \left(\sum_{t_i=0}^{t_i=t_f} s_6(t_i) - 0 \right)^2$ was minimized subject to the equations governing the model. This led to a value of zero (the Utopia point). The MNLMPC values of the control variables, u_1 and u_2 were 0.9999 and 0.3362. The control profiles u_1 and u_2 exhibited noise and this was remedied using the Savitzky-Golay filter to produce the smooth control profiles u_1sg and u_2sg . The MNLMPC profiles are shown in Figs 2a-2e. The presence of the branch point causes the MNLMPC calculations to attain the Utopia solution, validating the analysis of Sridhar (2024) [23].

Conclusions

Bifurcation analysis and multiobjective nonlinear control (MNLMPC) studies on an Acetaminophen Metabolism dynamic model. The bifurcation analysis revealed branch and limit points. The branch and limit points (which cause multiple steady-state solutions from a singular point) are very beneficial because they enable the Multiobjective nonlinear model predictive control calculations to converge to the Utopia point (the best possible solution) in the model. A combination of bifurcation analysis and Multiobjective Nonlinear Model Predictive Control (MNLMPC) for an Acetaminophen Metabolism dynamic model is the main contribution of this paper.

Data Availability Statement

All data used is presented in the paper

Conflict of Interest

The author, Dr. Lakshmi N Sridhar has no conflict of interest.

Acknowledgement

Dr. Sridhar thanks Dr. Carlos Ramirez and Dr. Suleiman for encouraging him to write single-author papers

References

1. Mutlib, A. E., Goosen, T. C., Bauman, J. N., Williams, J. A., Kulkarni, S., & Kostrubsky, S. (2006). Kinetics of acetaminophen glucuronidation by UDP-glucuronosyltransferases 1A1, 1A6, 1A9 and 2B15. Potential implications in acetaminophen– induced hepatotoxicity. *Chemical research in toxicology*, 19(5), 701-709.
2. Reed, M. C., Thomas, R. L., Pavisic, J., James, S. J., Ulrich, C. M., & Nijhout, H. F. (2008). A mathematical model of glutathione metabolism. *Theoretical biology and medical modelling*, 5(1), 8.
3. Reith, D., Medlicott, N. J., Kumara De Silva, R., Yang, L., Hickling, J., & Zacharias, M. (2009). Simultaneous modelling of the Michaelis-Menten kinetics of paracetamol sulphation and glucuronidation. *Clinical and Experimental Pharmacology and Physiology*, 36(1), 35-42.
4. Trinh, C. T., Wlaschin, A., & Srienc, F. (2009). Elementary mode analysis: a useful metabolic pathway analysis tool for characterizing cellular metabolism. *Applied microbiology and biotechnology*, 81(5), 813-826.
5. Ben-Shachar, R., Chen, Y., Luo, S., Hartman, C., Reed, M., & Nijhout, H. F. (2012). The biochemistry of acetaminophen hepatotoxicity and rescue: a mathematical model. *Theoretical biology and medical modelling*, 9(1), 55.
6. Remien, C. H., Adler, F. R., Waddoups, L., Box, T. D., & Sussman, N. L. (2012). Mathematical modeling of liver injury and dysfunction after acetaminophen overdose: early discrimination between survival and death. *Hepatology*, 56(2), 727-734.
7. Reddyhoff, D., Ward, J., Williams, D., Regan, S., & Webb, S. (2015). Timescale analysis of a mathematical model of acetaminophen metabolism and toxicity. *Journal of theoretical biology*, 386, 132-146.
8. Ghosh, A., Berger, I., Remien, C. H., & Mubayi, A. (2021). The role of alcohol consumption on acetaminophen induced liver injury: implications from a mathematical model. *Journal of Theoretical Biology*, 519, 110559.
9. Sankarraman, S. M. (2022). A computational approach on acetaminophen drug using degree-based topological indices and m-polynomials. *Biointerface Research in Applied Chemistry*, 12(6), 7249-7266.
10. Belmont-Díaz, J., Vázquez, C., Encalada, R., Moreno-Sánchez, R., Michels, P. A., & Saavedra, E. (2022). Metabolic control analysis for drug target selection against human diseases. In *Drug Target Selection and Validation* (pp. 201-226). Cham: Springer International Publishing.
11. Yoo, S. H., Lee, S. C., & Kim, S. B. (2023). Acetaminophen adsorption to spherical carbons hydrothermally synthesized from sucrose: experimental, molecular, and mathematical modeling studies. *Environmental Science and Pollution Research*, 30(17), 49703-49719.
12. Dichamp, J., Cellière, G., Ghallab, A., Hassan, R., Boissier, N., Hofmann, U., ... & Drasdo, D. (2023). In vitro to in vivo acetaminophen hepatotoxicity extrapolation using classical schemes, pharmacodynamic models and a multiscale spatial-temporal liver twin. *Frontiers in Bioengineering and Biotechnology*, 11, 1049564.
13. Zahwa, N., & Toaha, S. (2025). Optimal Control Strategies for Reducing Toxic Formation in Acetaminophen Metabolism. *Journal of Nonlinear Modeling and Analysis*, 7(5), 1830-1858.
14. Dhooge, A., Govaerts, W., & Kuznetsov, Y. A. (2003). MATCONT: a MATLAB package for numerical bifurcation analysis of ODEs. *ACM Transactions on Mathematical Software (TOMS)*, 29(2), 141-164.
15. Dhooge, A., Govaerts, W., Kuznetsov, Y. A., Mestrom, W., & Riet, A. M. (2003, March). Cl_matcont: a continuation toolbox in Matlab. In *Proceedings of the 2003 ACM symposium on Applied computing* (pp. 161-166).
16. Kuznetsov, Y. A. (1998). *Elements of applied bifurcation theory*. New York, NY: Springer New York.
17. Kuznetsov, Y. A. (2009). *Five lectures on numerical bifurcation analysis*. Utrecht University, NL.
18. Govaerts, W. J. (2000). *Numerical methods for bifurcations of dynamical equilibria*. Society for Industrial and Applied Mathematics.
19. Flores-Tlacuahuac, A., Morales, P., & Rivera-Toledo, M. (2012). Multiobjective nonlinear model predictive control of a class of chemical reactors. *Industrial & Engineering Chemistry Research*, 51(17), 5891-5899.
20. Hart, W. E., Laird, C. D., Watson, J. P., Woodruff, D. L., Hackebeil, G. A., Nicholson, B. L., & Siirola, J. D. (2017). *Pyomo-optimization modeling in python* (Vol. 67, p. 277). Berlin: Springer.
21. Wächter, A., Biegler, L. "On the implementation of an interior-point filter line-search algorithm for large-scale nonlinear programming". *Math. Program.* 106, 25–57 (2006).
22. Tawarmalani, M., & Sahinidis, N. V. (2005). A polyhedral branch-and-cut approach to global optimization. *Mathematical programming*, 103(2), 225-249.
23. Sridhar, L. N. (2024). *Coupling Bifurcation Analysis and Multiobjective Nonlinear Model Predictive Control*. *Austin Chem Eng*, 10(3), 1107.
24. Upreti, S. R. (2013). *Optimal control for chemical engineers* (p. 305). Taylor & Francis.

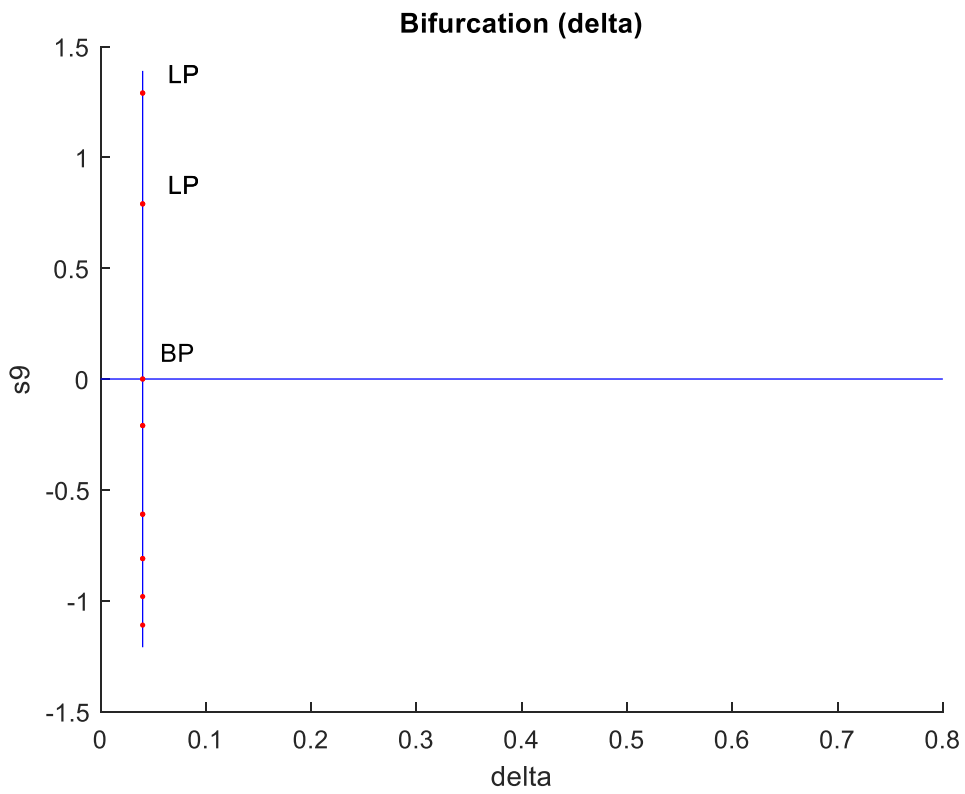


Figure 1a: Bifurcation Diagram is the Bifurcation Parameter

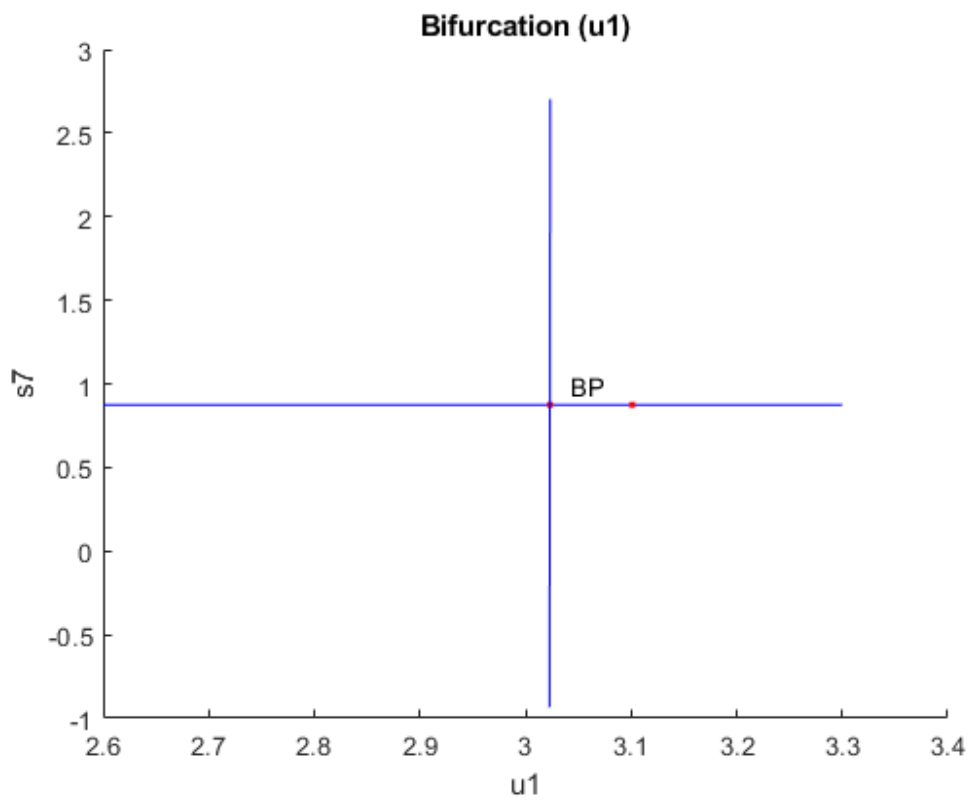


Figure 1b: Bifurcation Diagram with u1 as the Bifurcation Parameter

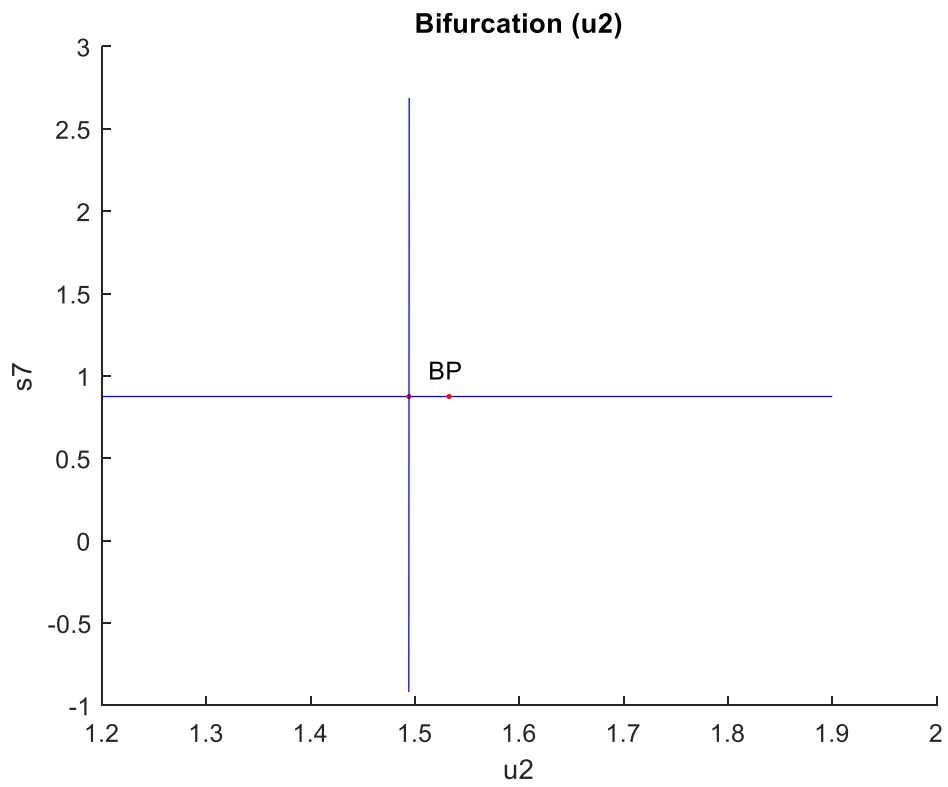


Figure 1c: Bifurcation Diagram With u_2 as the Bifurcation Parameter

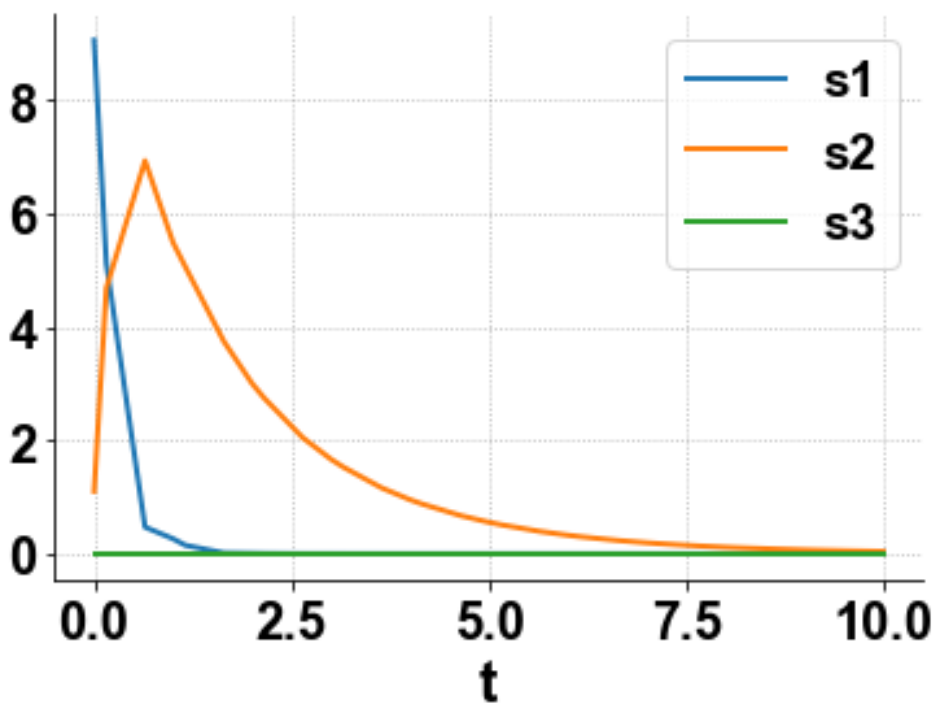


Figure 2a: MNLMPCC s_1, s_2, s_3

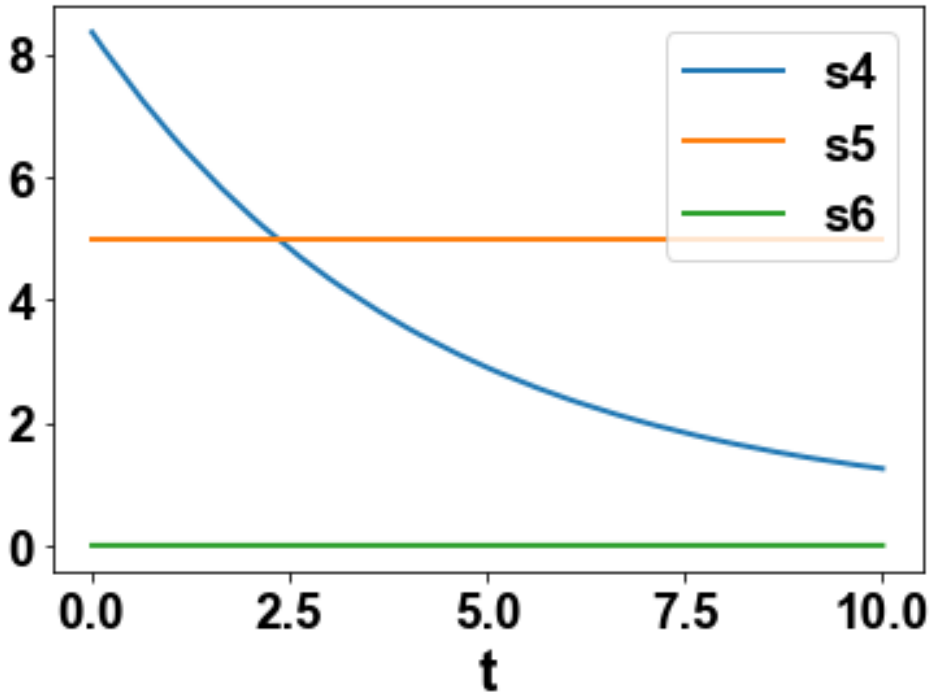


Figure 2b: MNLMPc s4, s4, s6

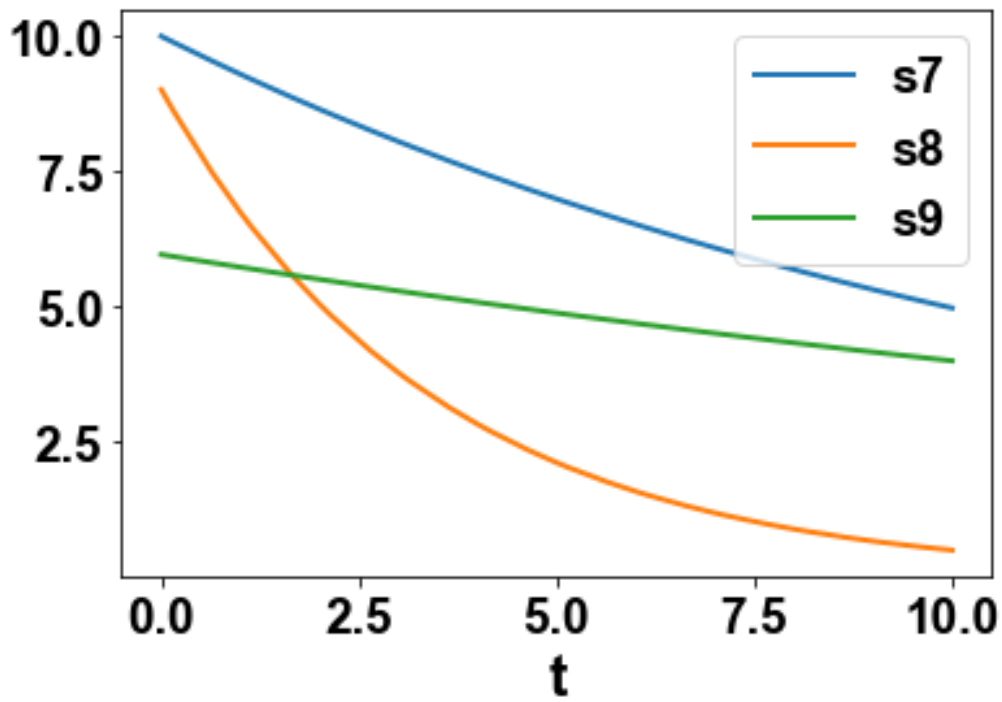


Figure 2c: MNLMPc s7, s8, s9

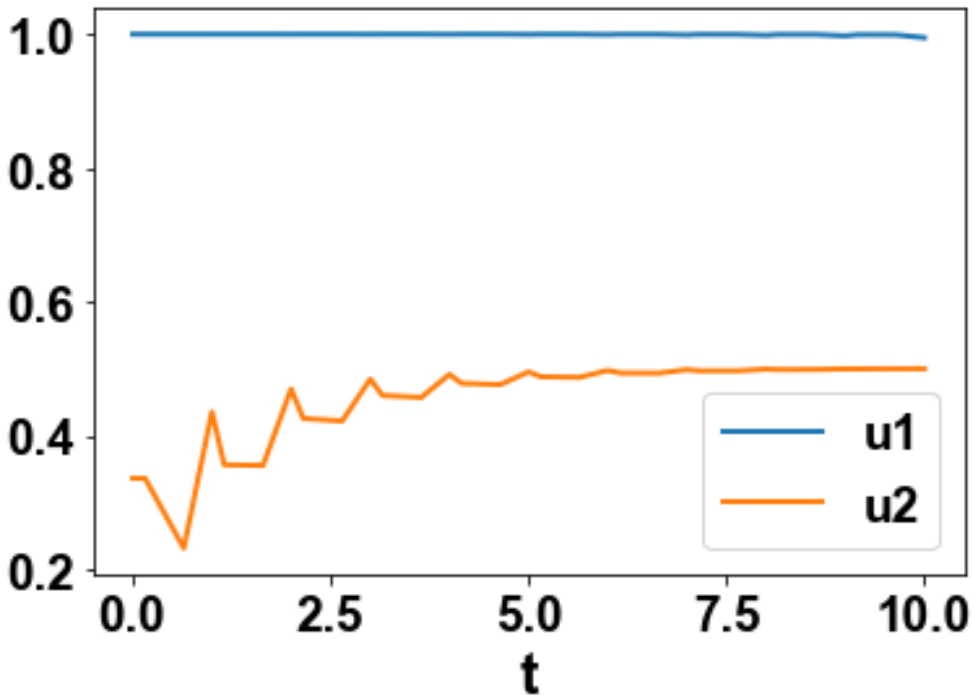


Figure 2d: MNLMP u_1, u_2

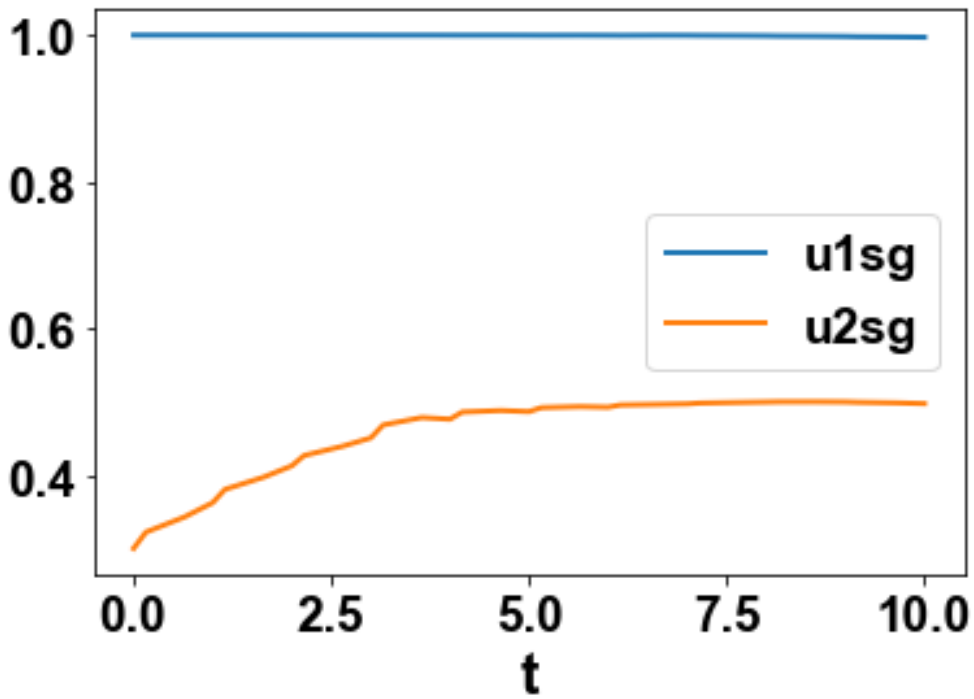


Figure 2e: MNLMP u_{1sg}, u_{2sg}